LETTERS

The magnetic nature of disk accretion onto black holes

Jon M. Miller[1], John Raymond[2], Andy Fabian[3], Danny Steeghs[2], Jeroen Homan[4], Chris Reynolds[5], Michiel van der Klis[6] & Rudy Wijnands[6]

Although disk accretion onto compact objects—white dwarfs, neutron stars and black holes—is central to much of high-energy astrophysics, the mechanisms that enable this process have remained observationally difficult to determine. Accretion disks must transfer angular momentum in order for matter to travel radially inward onto the compact object[1]. Internal viscosity from magnetic processes[1–4] and disk winds[5] can both in principle transfer angular momentum, but hitherto we lacked evidence that either occurs. Here we report that an X-ray-absorbing wind discovered in an observation of the stellar-mass black hole binary GRO J1655−40 (ref. 6) must be powered by a magnetic process that can also drive accretion through the disk. Detailed spectral analysis and modelling of the wind shows that it can only be powered by pressure generated by magnetic viscosity internal to the disk or magnetocentrifugal forces. This result demonstrates that disk accretion onto black holes is a fundamentally magnetic process.

To study the nature of disk accretion onto black holes, we observed the transient source GRO J1655−40 with the Chandra X-ray Observatory for 63.5 ks starting on 1 April 2005 at 12:41:44 (terrestrial time, TT), during an X-ray bright phase of its 2005 outburst. GRO J1655−40 is a binary system at a distance of 3.2 kpc that harbours a black hole with a mass of $7.0M_{\odot}$ ($M_{\odot}$ is the solar mass), which accretes from an F3 IV–F6 IV star with a mass of $2.3M_{\odot}$ in a 2.6-day orbit[6]. The inner disk is viewed at an inclination of 67–85° (nearly edge-on)[6,7]. Using Chandra, we obtained a robust high-resolution X-ray spectrum of GRO J1655−40 in the soft X-ray band (Fig. 1).

It is common to decompose the broad-band spectra of stellar-mass black holes into disk blackbody and power-law components. Assuming the standard equivalent neutral hydrogen absorption[8] along the line of sight to GRO J1655−40 (equivalent neutral hydrogen column density $N_{\rm H} = 7.4 \times 10^{21}$ atoms cm^{-2}), this spectral model gives a disk temperature of $kT = 1.34(1)$ keV (where k is Boltzmann's constant, and numbers in parentheses indicate the error in the last significant digit) and a photon power-law index of $\Gamma = 3.54(1)$ in the 1.2–19 Å range, and a total flux of $4.70(5) \times 10^{-8}$ erg cm^{-2} s^{-1} (unabsorbed). This flux implies a luminosity of $L = 3.3 \times 10^{37}$ erg s^{-1} for a distance from Earth of $d = 3.2$ kpc, or 4% of the Eddington limit for a $7M_{\odot}$ black hole. The disk contributes 65% of the unabsorbed flux.

The HETGS (High Energy Transmission Grating Spectrometer) spectra of GRO J1655−40 contain 90 absorption lines significant at the 5σ level of confidence or higher. We can confidently identify 76 of these lines with resonance lines expected from over 32 charge states. The properties of these lines were measured with simple gaussian line functions and local continuum models. Line centroid wavelengths and oscillator strengths were taken from a set of standard references[9–11]. Two findings demand that the absorption arises in a disk-driven wind. First, the lines show blueshifts in the 300–1,600 km s^{-1} range, indicating a flow into our line of sight (Figs 1 and 2, and Supplementary Information). Second, the spectra contain no strong emission lines; this fact signals that the absorbing gas is mostly equatorial along the plane of the disk.

To understand better the nature of the wind, we constructed a number of photoionized plasma models based on the methodology and atomic physics packages described in earlier work[12,13]. (The models used in this work differ only in that new dielectronic recombination rates for Fe and Ni were used to more accurately describe L-shell ions[14].) These models describe a gas in photoionization equilibrium, with heating by photoionization and Compton

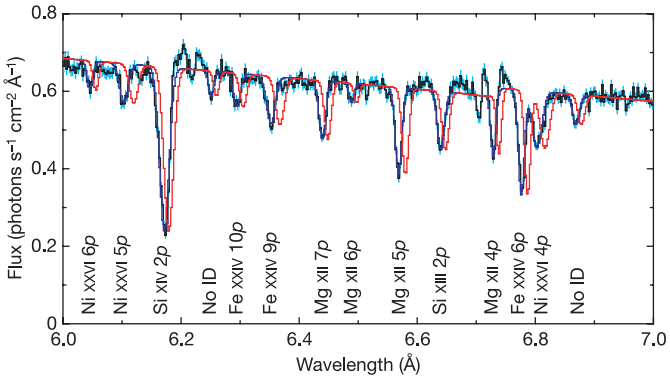

Figure 1 | A small part of the disk wind spectrum observed in GRO J1655−40 with Chandra. The best-fit phenomenological model is shown in blue. The model in red plots the natural line wavelengths, to illustrate that the observed absorption is blueshifted. The errors shown are 1σ statistical errors on the photon flux. To obtain this high-resolution spectrum, the Chandra HETGS was used to disperse the X-ray flux onto the Advanced CCD Imaging Spectrometer (ACIS), which was operated in 'continuous-clocking' mode. The data reduction and preparation were performed using the latest version of the standard Chandra packages (CIAO), and a procedure typical for this instrumental configuration[13]. The spectra presented in this work were produced by adding the first-order spectra from the HETGS medium-energy grating (MEG) at a resolution of 0.005 Å per bin, and the first-order spectra from the high-energy grating (HEG) at a resolution of 0.0025 Å per bin. The HEG spectrum was used to characterize the 1–11 Å band, and the MEG spectrum was used to characterize the 11–19 Å band. The continuum emission was characterized using the HEG spectrum. All spectral fits were made using the ISIS[29] spectral fitting package.

[1]Department of Astronomy, University of Michigan, 500 Church Street, Ann Arbor, Michigan 48109, USA. [2]Harvard-Smithsonian Center for Astrophysics, 60 Garden Street, Cambridge, Massachusetts 02138, USA. [3]Institute of Astronomy, University of Cambridge, Cambridge CB3 OHA, UK. [4]Kavli Institute for Astrophysics and Space Research, Massachusetts Institute of Technology, 77 Massachusetts Avenue, Cambridge, Massachusetts 02139, USA. [5]Department of Astronomy, University of Maryland, College Park, Maryland 20742, USA. [6]Astronomical Institute Anton Pannekoek, University of Amsterdam, Kruislaan 403, 1098 SJ Amsterdam, The Netherlands.

scattering and cooling by line and continuum emission and Compton scattering. The predicted ionization state of the gas is combined with a curve of growth[15] for a chosen velocity width to determine line equivalent widths using Voigt profiles. The code accounts for line blends self-consistently. A standard set of elemental abundances are used in the code[16]. The illuminating spectrum is taken to be the composite thermal and non-thermal continuum spectrum described briefly above.

The observed spectrum is consistent with absorption in a constant-density slab with a thickness of approximately 2.5×10^8 cm and a number density of $n = 5.6 \times 10^{15}$ atoms cm^{-3} at a mean distance of 4.8×10^8 cm from the black hole. This translates to approximately $200R_{\rm Schw}$ (where the Schwarzschild radius $R_{\rm Schw} = 2GM_{\rm BH}/c^2$, with G the gravitational constant, $M_{\rm BH}$ the black hole mass, and c the velocity of light); the component of the wind velocity in our line of sight is much slower than the local virial velocity. The temperature of the gas is $(0.2–1.0) \times 10^6$ K. An intrinsic full-width at half-maximum (FWHM) of 300 km s^{-1} matches the observed lines which are not saturated (Fig. 2 and Supplementary Information). An important feature of this wind is that it is highly ionized: $\log \xi = \log(L_{\rm X}/nr^2) =$ 4.2–4.7 (where ξ is the ionization parameter, $L_{\rm X}$ is X-ray luminosity, n is density, and r is the radius from the ionizing source).

The data permit strong independent constraints on the geometry and extent of the wind absorption. An inner radial extent of $10^{7.5}$ cm is set by the density at which Fe XXIII lines are produced. At smaller radii, the ionization parameter requires a density so large that the metastable $2s2p^3$ P level of Fe XXIII would be populated, producing lines that are not observed. An outer radial extent of $10^{9.5}$ cm is set by dilution and line ratios. At larger radii, the thickness of the absorbing gas becomes large compared to the distance, so $1/r^2$ dilution of the radiation field makes it impossible to get enough total column at high enough ionization parameter. A lower limit of 6° on the height of the gas above the disk midplane comes from the fact that the line of sight must pass over the outer edge of the disk[17]. An upper limit on the vertical extent comes from the lack of emission features. A Monte Carlo simulation for a cascade resulting from absorption in the $2s$–$4p$ line of Fe XXIV predicts a $2p$–$3s$ emission line with equivalent width $0.65 \times 28\Omega/4\pi = 18\Omega/4\pi$ mÅ (where Ω is the solid angle covering factor). An upper limit of a 2 mÅ to such a feature implies an upper limit of about 12° to the vertical extent of the absorbing gas.

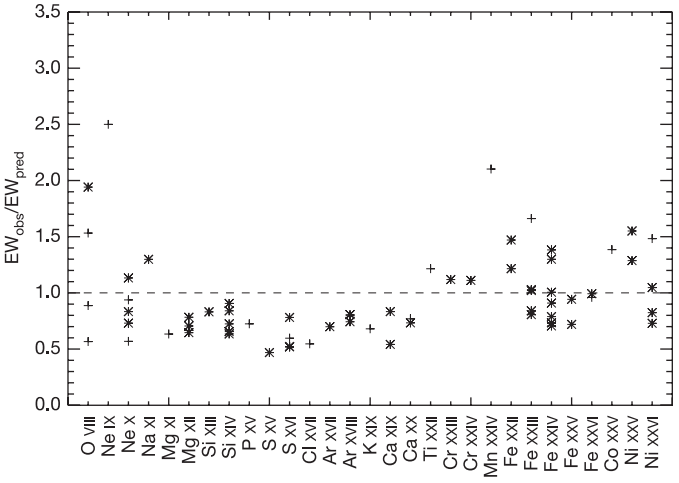

Figure 2 | Comparison to the data of the best model for the disk wind in GRO J1655−40. The plot shows the ratio of the absorption line equivalent widths measured in GRO J1655−40, EW$_{\rm obs}$, to the equivalent widths predicted by the photoionization model that best describes the disk wind, EW$_{\rm pred}$. The model assumes internal velocity widths of 300 km s^{-1}. Revised solar abundances[16] are adequate to describe the elements between Na and K (inclusive). Abundances of twice the revised solar value are required to describe the lines observed from other elements. For visual clarity, stronger lines are marked with stars, and weaker lines with crosses. The full spectrum of GRO J1655−40 and the measured properties of the absorption lines are detailed in the Supplementary Information.

The properties of thermally driven winds have been studied, especially within the context of outer accretion disks being illuminated by a central X-ray source[18]. In such cases, it is possible to define a critical radius $R_{\rm C} = (1.0 \times 10^{10}) \times (M_{\rm BH}/M_\odot)/(T_{\rm C8})$ cm, and a wind may occur for any $R/R_{\rm C} > 0.1$ (where $T_{\rm C8}$ is the gas temperature in units of 10^8 K). On the basis of temperatures derived from our photoionization models, the smallest possible value of $R_{\rm C}$ for the wind observed in GRO J1655−40 is 7×10^{12} cm. Thus, the minimum radius at which a disk wind can be thermally driven is approximately two orders of magnitude greater than is plausible in GRO J1655−40. Similar results are obtained when our results are compared to new models for the winds in active galactic nuclei (AGN) such as NGC 3783 (ref. 19).

The wind observed is too highly ionized to be driven by radiation pressure. The overwhelming majority of absorption lines observed are from He-like and H-like species, which means that there is little ultraviolet opacity in the wind by which momentum may be transferred. At ionization parameters of $\xi > 10^3$, models for line-driven winds in AGN indicate that ultraviolet emission lines provide no additional driving force[20]. Moreover, our photoionization code measures radiation pressure as the momentum of the photons absorbed, which is comparable to the electron scattering radiation pressure, and even together these effects fall far short of producing the observed momentum flux in the wind.

Given that thermal and radiative driving fail by orders of magnitude, magnetic driving of the wind in GRO J1655−40 is the only plausible mechanism remaining. Our model implies a mass loss rate in the wind of $\dot{m}_{\rm w} = 3.5 \times 10^{17}$ g s^{-1} or approximately 0.5 g cm^{-2} s^{-1}. For a typical blueshift of 500 km s^{-1}, this translates into a kinetic energy flux of 6.3×10^{14} erg cm^{-2} s^{-1}. An angle of 9° above the disk midplane at a radius of 4.8×10^8 cm from the black hole corresponds to a height of $Z = 0.15r$; an energy flux of 2.0×10^{16} erg cm^{-2} s^{-1} is required to lift the gas to that height. The luminosity of the central engine as derived from fits to the continuum implies a mass accretion rate of $\dot{m}_{\rm a} = 3.7 \times 10^{17}$ g s^{-1} for an accretion efficiency of 10%. The viscous energy flux dissipated is given by $3GM_{\rm BH}\dot{m}_{\rm a}/4\pi r^3 = 2.3 \times 10^{18}$ erg cm^{-2} s^{-1}. Recent simulations show that the magnetorotational instability[2,3,4] can not only drive turbulence, viscosity and accretion through a disk, but can transmit 25% of the magnetic energy flux vertically out of the disk[21] and drive a wind. In the case of GRO J1655−40, 25% of the viscous energy flux is comparable to the flux required to drive the wind to infinity. The wind outflow velocity and mass outflow rate are remarkably similar to predictions resulting from simulations of magnetically driven winds from magneto-rotational instability (MRI) disks[22].

It is also possible that the wind is driven by magnetocentrifugal forces[5]. The absorption spectrum contains no information about velocities tangential to our line of sight. Theoretical models show that largely equatorial winds can arise via magnetocentrifugal driving when the magnetic field vector makes a small angle to the disk plane[23]; however, recent simulations suggest that it is difficult to maintain the poloidal magnetic field required in a wind with a large mass outflow[22]. Given that the wind arises in a disk that is almost certainly keplerian, however, magnetocentrifugal driving cannot be discounted. The winds in some young stars (FU Orionis class) are driven by magnetocentrifugal forces[24]. Tapping into the rotational velocity of the disk would help to expel the wind to infinity. Although internal magnetic viscosity and magnetic winds are sometimes posited as complete and separate processes, the most physically realistic scenario may be one in which both processes act to drive disk accretion and outflows.

Winds are commonly observed in accreting compact objects; however, GRO J1655−40 is the first case wherein it is clear that the

wind must be launched from the disk (not the companion star) and must be driven primarily by magnetic processes (not thermal and radiative pressure). An X-ray wind with some similarities to those in AGN was detected in the accreting neutron star binary Circinus X-1 (ref. 25); however, in Circinus X-1 contributions from a massive companion star cannot be ruled out, and the wind could be driven by thermal and radiation pressure[25]. A wind more certainly tied to the disk was detected in the black hole binary GX 339−4, but too few lines were detected to constrain the driving mechanism[13]. Though radiative driving may be important in most white dwarf systems, there is at least one system where it may be inadequate[26]. Similarly, theoretical considerations suggest that magnetocentrifugal forces are important in AGN winds[27,28], but present data do not yet require or rule out these effects. Our results therefore represent a rare and crucial insight into the nature of the processes that drive disk accretion in black holes.

Magnetic pressure supplied by the disk provides a natural means of driving the highly ionized winds observed in many accreting stellar-mass black holes and neutron stars, and may play a role in driving the hottest winds observed in AGN. Indeed, winds and jets are ubiquitous features in accretion-powered astrophysics, and the role of magnetic processes revealed in GRO J1655−40 gives a broad observational insight into the physical coupling between inflows and outflows in accreting compact objects.

Received 22 December 2005; accepted 10 May 2006.

1. Shakura, N. I. & Sunyaev, R. A. Black holes in binary systems. Observational appearance. *Astron. Astrophys.* **24,** 337–355 (1973).
2. Balbus, S. A. & Hawley, J. F. A powerful local shear instability in weakly magnetized disks. *Astrophys. J.* **376,** 214–233 (1991).
3. Hawley, J. F., Gammie, C. F. & Balbus, S. A. Local three-dimensional magneto-hydrodynamic solutions of accretion disks. *Astrophys. J.* **440,** 742–763 (1995).
4. Balbus, S. A. & Hawley, J. F. Instability, turbulence, and enhanced transport in accretion disks. *Rev. Mod. Phys.* **70,** 1–53 (1998).
5. Blandford, R. D. & Payne, D. G. Hydromagnetic flows from accretion disks and the production of radio jets. *Mon. Not. R. Astron. Soc.* **199,** 883–903 (1982).
6. Orosz, J. & Bailyn, C. D. Optical observations of GRO J1655−40 in quiescence. I. A precise mass for the black hole primary. *Astrophys. J.* **477,** 876–896 (1997).
7. Hjellming, R. M. & Rupen, M. P. Episodic ejection of relativistic jets by the X-ray transient GRO J1655−40. *Nature* **375,** 464–468 (1995).
8. Dickey, J. M. & Lockman, F. J. H I in the Galaxy. *Annu. Rev. Astron. Astrophys.* **28,** 215–261 (1990).
9. Verner, D. A., Verner, E. M. & Ferland, G. J. Atomic data for permitted resonance lines of atoms and ions from H to Si, and S, Ar, Ca, and Fe. *Atom. Data Nucl. Data Tables* **64,** 11–180 (1996).
10. The NIST Atomic Spectra Database, Standard Reference Database 78. ⟨http://physics.nist.gov/cgi-bin/AtData/main.asd⟩ (2005).
11. Nahar, S. & Pradhan, A. K. Atomic data from the Iron Project. XXXV. Relativistic fine structure oscillator strengths for Fe XXIV and Fe XXV. *Astron. Astrophys. Suppl.* **135,** 347–357 (1999).
12. Raymond, J. A model of an X-ray-illuminated accretion disk and corona. *Astrophys. J.* **412,** 267–277 (1993).
13. Miller, J. M. *et al.* Chandra/HETGS spectroscopy of the Galactic black hole GX 399−4: A relativistic iron emission line and evidence for a Seyfert-like warm absorber. *Astrophys. J.* **601,** 450–465 (2004).
14. Colgan, J., Pindzola, M. S. & Badnell, N. R. Dielectronic recombination data for dynamic finite-density plasmas. V: the lithium isoelectronic sequence. *Astron. Astrophys.* **417,** 1183–1188 (2004).
15. Spitzer, L. *Physical Processes in the Interstellar Medium* (Wiley, New York, 1978).
16. Grevesse, N. & Sauval, A. J. in *Solar Composition and its Evolution–from Core to Corona* (eds Frölich, C., Huber, M. C. E., Solanski, S. K. & von Steiger, R.) 161–174 (Kluwer, Dordrecht, 1998).
17. Vrtilek, S. *et al.* Observations of Cygnus X-2 with IUE—Ultraviolet results from a multi-wavelength campaign. *Astron. Astrophys.* **234,** 162–173 (1990).
18. Begelman, M. C., McKee, C. F. & Shields, G. A. Compton heated winds and coronae above accretion disks. II Dynamics. *Astrophys. J.* **271,** 70–89 (1983).
19. Chelouche, D. & Netzer, H. Dynamical and spectral modeling of the ionized gas and nuclear environment in NGC 3783. *Astrophys. J.* **625,** 95–107 (2005).
20. Proga, D., Stone, J. M. & Kallman, T. R. Dynamics of line-driven winds in active galactic nuclei. *Astrophys. J.* **543,** 686–696 (2000).
21. Miller, K. A. & Stone, J. M. The formation and structure of a strongly magnetized corona above a weakly magnetized accretion disk. *Astrophys. J.* **534,** 398–419 (2000).
22. Proga, D. Numerical simulations of mass outflows driven from accretion disks by radiation and magnetic forces. *Astrophys. J.* **585,** 406–417 (2003).
23. Spruit, H. C. in *Physical Processes in Binary Stars* (eds Wijers, R. A. M. J., Davies, M. B. & Tout, C. A.) 249–286 (NATO ASI Ser., Kluwer, Dordrecht, 1996).
24. Calvet, N., Hartmann, L. & Kenyon, S. J. Mass loss from pre-main-sequence accretion disks. I—The accelerating wind of FU Orionis. *Astrophys. J.* **402,** 623–634 (1993).
25. Schulz, N. S. & Brandt, W. N. Variability of the X-ray P Cygni line profiles from Cicinus X-1 near zero phase. *Astrophys. J.* **572,** 972–983 (2002).
26. Mauche, C. W. & Raymond, J. C. Extreme Ultraviolet Explorer observations of OY Carinae in superoutburst. *Astrophys. J.* **541,** 924–936 (2000).
27. Konigl, A. & Kartje, J. F. Disk-driven hydromagnetic winds as a key ingredient of active galactic nuclei unification schemes. *Astrophys. J.* **434,** 446–467 (1994).
28. Everett, J. E. Radiative transfer and acceleration in magnetocentrifugal winds. *Astrophys. J.* **631,** 689–706 (2005).
29. Houck, J. C. & Denicola, L. A. ISIS: An interactive spectral interpretation system for high resolution X-ray spectroscopy. *Astron. Soc. Pacif. Conf. Proc.* **216,** 591–594 (2000).

Supplementary Information is linked to the online version of the paper at www.nature.com/nature.

Acknowledgements We acknowledge conversations with N. Calvet, L. Hartmann, D. Proga and M. Rupen. We are indebted to A. Prestwich, H. Tananbaum and the Chandra staff for help in making this observation possible. We thank B. Lauritsen for editorial insights. This work was supported by NASA through the Chandra guest observer programme (J.M.M.).

Author Contributions J.M.M. analysed the Chandra data and wrote most of the paper. J.R. developed the photoionization model. J.M.M., J.R., A.F. and C.R. developed the interpretation of the data. D.S., J.H., M.K. and R.W. contributed insights on X-ray binaries and/or made supporting observations with other instruments. All others discussed the work at length, and contributed to the manuscript.

Author Information Reprints and permissions information is available at npg.nature.com/reprintsandpermissions. The authors declare no competing financial interests. Correspondence and requests for materials should be addressed to J.M.M. (jonmm@umich.edu).